TWO-DIMENSIONAL SUPERSONIC WING THEORY

By Walter G. Vincenti

Ames Aeronautical Laboratory

INTRODUCTION

The problem of an airfoil section in two-dimensional supersonic flow, which is fundamental to a consideration of other, more general wing problems in supersonic flight, was first treated theoretically in a paper by Ackeret published in Germany in 1925. Shortly thereafter - in 1928 - experimental results were reported in England by Stanton. As a result of the work of these and a number of later investigators, the fundamentals of the problem were well, though perhaps not widely, understood before the beginning of World War II. During the wartime and postwar periods, detailed advances in both theory and experiment have been made, as well as increased application of the available knowledge, usually on classified projects. The fundamental ideas in the field, however, can be discussed almost completely in terms of results available prior to 1940.

FUNDAMENTAL CONSIDERATIONS OF SUPERSONIC FLOW

Before proceeding to the discussion of the theory, it is desirable to review briefly the fundamental difference between subsonic and supersonic flow (references 1 to 4). This difference is illustrated in figure 1, which shows the wave pattern set up by a disturbance point in both a steady subsonic stream and supersonic stream. In either case, if the disturbances from the point are small, each elementary disturbance is propagated spherically at the speed of sound relative to the moving stream. Because of the motion of the stream, however, the center of each elementary sphere is at the same time carried downstream relative to the original source of the disturbance. If the speed of the stream is less than the speed of sound, as shown on the left in figure 1, the elementary disturbances will travel upstream against the flow faster than their centers are swept downstream. As a result, the disturbances move ahead of their source and affect all parts of the flow field. In a supersonic stream, as shown on the right in this figure, the centers of the disturbance spheres are carried downstream faster than the disturbance itself can be propagated forward. As a result, all disturbances in the supersonic stream are confined to the interior of a cone known as the Mach cone. The flow outside this region is, so to speak, unaware of the presence of any disturbance. It is apparent that the greater the supersonic speed, the smaller the included angle at the apex of the Mach cone. These simple considerations must be modified somewhat if the disturbances are not small; however, the results serve as a reasonable first approximation in most actual cases.

The concept of the Mach cone has important implications with regard to the applicability of two-dimensional theory and data to parts of three-dimensional wings. The relationship of this concept to three-dimensional wings is illustrated in figure 2. In the case of the straight wing, for example, the effect of the finite span of the wing is confined approximately to conical regions extending downstream from the leading edge of each tip. The flow over the remainder of the wing (shaded area) is not influenced by the presence of the tips and this shaded area is thus a region of two-dimensional flow. For the more complex plan forms shown, the flow over the shaded regions is similarly unaffected by the presence of the tips and, for these examples, of the root of the wing as well. Within these regions the flow can be treated as essentially two-dimensional by utilizing the components of the flow quantities and deflection angles normal to the swept straight-line elements which generate the wing surface (reference 5).

FLOW FIELD ABOUT AN AIRFOIL SECTION

With this background, consider the general character of the two-dimensional flow field about an airfoil section at supersonic speed. Figure 3 is a diagram of the idealized, inviscid flow around a simple, double-wedge section at angle of attack for a free-stream Mach number of approximately 2. The pattern shown is that predicted by theory when the local velocity in the flow field is everywhere supersonic. In accordance with the previous considerations of supersonic flow, the oncoming stream (fig. 3) continues undisturbed until it reaches the region of influence of the airfoil. Within this region the flow changes are of two general kinds. When the flow is turned around a concave corner, as on the lower surface at the leading edge, a compression takes place. When the flow is turned around a convex corner, as on the upper surface at the same location, an expansion results. The compression from the concave corner takes place discontinuously through an oblique shock wave with an accompanying dissipation of energy - that is, with an increase in entropy. The expansion takes place continuously and isentropically in a fan-shaped region originating at the convex corner. Thus, if the flow is along a streamline some distance above the present airfoil, the air first undergoes reductions in pressure through two successive expansion regions, one originating at the leading edge and one at the ridge line, and is then recompressed by a shock wave originating at the trailing edge. The air beneath the lower surface is, in the same general manner, first compressed through a shock wave and then successively expanded through two expansion regions. It is interesting to note that along the surface of the airfoil itself the expansions as well as the compressions take place discontinuously. Thus, contrary to the condition which would exist in subsonic flow, there is no stagnation point in the vicinity of the leading edge and no tendency toward an infinite velocity at the sharp convex corners.

As the angle of attack of the airfoil is changed, the flow pattern will, of course, change correspondingly. In particular, the flow disturbance on a given surface at the leading or trailing edge will change from an expansion to a compression, or vice versa, as the required deflection of the stream is altered. Of more importance, as the angle of attack is increased, a condition is eventually reached in which the flow behind the shock wave at the leading edge is no longer supersonic but becomes subsonic instead. At a slightly higher angle of attack, the wave detaches and moves forward of the airfoil. These latter effects also occur at a given angle of attack when the Mach number is reduced toward unity. Once such changes have taken place, the entire character of the flow pattern is altered and the purely supersonic considerations of the foregoing discussion no longer apply.

For simplicity, the discussion herein has been carried out in terms of a simple, flat-sided section. The same considerations apply to a curved profile so long as the leading edge is sharp, except that in such a case the expansion along the convex curved surface takes place gradually rather than discontinuously. (The restriction of the discussion to airfoils with a sharp leading edge is of no serious consequence, since an edge of this type appears desirable for optimum performance in the two-dimensional case when the velocity is more than slightly supersonic.)

METHODS OF ANALYSIS

Several theoretical methods are available for determining the characteristics of an airfoil in a two-dimensional supersonic flow. The methods all assume that the fluid is inviscid, that the leading and trailing edges of the airfoil are sharp, that any shock waves originating from these edges are attached to the airfoil, and that the flow behind the leading-edge shock wave is supersonic. They differ only in the degree of mathematical accuracy involved. In order of decreasing accuracy, the methods may be described as the shock-expansion theory, the second-order theory, and the linear (or first-order) theory.

Shock-Expansion Theory

The shock-expansion method follows directly from the application to the airfoil problem of known analytical results for an oblique shock wave and an expansion region (references 1 to 3 and 6 to 9). From simple considerations of momentum, energy, and continuity, the change in pressure and Mach number across a single shock wave can be calculated in terms of the Mach number of the oncoming flow and the angle of deflection of the flow in passing through the wave. Similar results can be obtained for an isolated expansion region. On the basis of these results together with the assumption that interaction effects between the individual shock waves and expansion regions are negligible, the pressure distribution over the airfoil surface can be calculated by a step-by-step procedure beginning at the leading edge and proceeding rearward (references 10 and 11). For example, on the lower surface of the double-wedge section in figure 3, if the free-stream Mach number and the deflection angle at the leading edge are known, the pressure and Mach number on the forward lower surface can be found from the equations for an oblique shock wave. By use of these quantities to provide the initial conditions for the flow approaching the ridge line, the pressure on the rear lower surface can then be found from the known results for an expansion. Because of the nature of the equations for an expansion, the procedure applies equally well to a section with a curved profile. Once the complete pressure distribution is known, the lift, pitching moment, and pressure drag of the airfoil are determined by graphical or numerical integration.

As compared with the theories to be discussed later, the shock-expansion method has the advantage of greater mathematical accuracy; in fact, in instances for which the assumption of no effective interference between the shock waves and expansion regions is satisfied, the method provides the complete inviscid solution to the problem. (The case illustrated in figure 3 can be shown to be of this type since the regions of flow influenced by the eventual intersections of the different disturbances lie completely downstream of the airfoil.) In other instances, notably on airfoils with curved surfaces, some interference does occur with a resulting approximation in the theory. The main disadvantage of the method, however, is that no analytical expressions are provided for the section characteristics, a separate set of calculations being required for each airfoil at each angle of attack.

Second-Order and Linear Theories

The disadvantage of the shock-expansion theory is overcome, at the expense of further approximation, by the second-order and linear theories (references 12 to 15). The relationship upon which these theories are based is given as equation (1) in figure 4. This equation, which is derived by series approximation to the complete equations for two-dimensional supersonic flow, expresses the pressure coefficient P at any point on the airfoil in terms of ascending powers of the local deflection angle η. The coefficients of the terms in the series are functions primarily of the free-stream Mach number M_0 and, secondarily of the ratio of the specific heats of the gas γ. By proper definition of the sign of the angle η - positive when the surface is facing toward the oncoming free stream and negative when facing away from the oncoming free stream (see diagram in fig. 4) - and by limitation of the power series to the first two terms, the same equation can be made to serve for both a compression and an expansion. This result illustrates the fact that in a given supersonic stream the pressure at a point on an airfoil in two-dimensional flow is, to the second order of approximation, determined solely by the local inclination of the airfoil surface. This is contrary to the situation in subsonic theory, in which the conditions at one point on an airfoil section depend, even to the first order, upon conditions at every other point.

On the basis of the foregoing simple result for the surface pressure, general second-order expressions for the lift, pitching-moment, and pressure-drag characteristics of any airfoil section can be obtained by direct integration. The final equations involve the coefficients C_1 and C_2, the angle of attack of the airfoil, and certain simple integrals which depend upon the airfoil shape only. These equations have been worked out in their most general form by Lock (references 15 and 8). For cases in which the shape of the airfoil can be expressed analytically, the integrals involved are readily evaluated to obtain direct equations for the airfoil characteristics in terms of the parameters which define the profile. These results are especially useful in studying the effects of systematic variation in thickness and camber for families of sections.

When both the terms C_1 and C_2 are retained, the general equations (see fig. 4) constitute the second-order theory. If the coefficient C_2 is in all cases set equal to zero, a linear (or first-order) theory is obtained. This latter approximation, which is sufficient for many purposes, is also known as the Ackeret theory since the linear theory was first proposed by Ackeret in his original treatment of the supersonic airfoil problem (reference 12). This elementary theory leads to certain exceedingly simple results. It indicates, for example, that the aerodynamic center of the airfoil is at midchord irrespective of the shape of the section and that the minimum pressure drag for a family of sections of given thickness distribution varies as the square of the thickness ratio. The second-order approximation, which modifies these results somewhat, was developed by Busemann (reference 14) at a later date when it was found that certain of the first-order results were not in complete accord with experiment. It is interesting to note, however, that even to the second order the lift-curve slope (per radian) for any airfoil section has the simple value of $2C_1$ or $\frac{4}{\sqrt{M_o^2 - 1}}$.

COMPARISON BETWEEN THEORY AND EXPERIMENT

Since the various theoretical methods have been reviewed, a comparison of the theoretical and experimental results for specific airfoils can now be made.

Pressure Distribution

Of first interest is an examination of a typical pressure distribution. Calculated and measured results are shown in figure 5 for a 10-percent-thick symmetrical, biconvex section at a Mach number of 2.13 and an angle of attack of 10^o. The local pressure is plotted in coefficient form as a function of the chordwise position; positive pressures are plotted below the horizontal axis and negative pressures, above. The pressure distributions calculated by the three theories are indicated by different lines in the figure. Experimental data obtained, as part of an extensive investigation, by Ferri (reference 16) are shown as individual points.

A noticeable improvement is seen in the accuracy of the theoretical calculations in going from the linear to the more refined theories. Over most of the section, both the second-order and shock-expansion theories show reasonable agreement with experiment although the check is slightly better when the shock-expansion theory is used. Over the rear 40 percent of the upper surface, however, the experimental pressures depart noticeably from the values given by any of the theories.

The discrepancy between the theoretical pressure distributions calculated by the linear theory and those calculated by the more precise theories has, curiously enough, little effect upon the value of the integrated lift. In fact, the area between the curves for the upper and lower surfaces, which gives a representation of the lift, is exactly the same for the linear and second-order theories. In other words, these two theories, although they disagree in chordwise lift distribution, agree in the value of the total lift for the present section. It is apparent from the difference in lift distribution, however, that the second-order theory gives a position of the center of pressure (or aerodynamic center) forward of that predicted by the linear theory. (The discrepancies noted between the various theories would, of course, be smaller for thinner airfoils and at lower angles of attack.)

The failure of even the higher-order theories to predict the pressure distribution over the rear part of the upper surface is known to be due to shock-wave, boundary-layer interaction (reference 16). As was previously indicated (see fig. 3), the idealized inviscid flow over a lifting airfoil section is characterized by an oblique compression wave originating on the upper surface at the trailing edge. In the real, viscous fluid the flow pattern is modified by an interaction between this trailing wave and the boundary layer on the airfoil surface. The boundary layer separates from the upper surface some distance ahead of the trailing edge, with the formation of a weak compression wave at the separation point and a consequent increase in pressure between this point and the trailing edge.

The difference between the pressure distributions shown herein and those characteristic of an airfoil in subsonic flow is apparent. Here, the pressures on both surfaces of the section decrease progressively toward the trailing edge with no pressure recovery such as that which occurs in the subsonic case. This lack of pressure recovery over the rear of the section at supersonic speeds gives rise, even in the theoretical inviscid flow, to an appreciable pressure drag. In the subsonic case the drag in a two-dimensional inviscid flow is, of course, exactly zero.

Over-All Aerodynamic Characteristics

With the foregoing results in mind, consider the over-all characteristics of a typical airfoil. Figure 6 presents theoretical and experimental lift and moment results, at the same Mach number as before, for a cambered, double-wedge airfoil of 6.3 percent thickness. A straight-sided airfoil was chosen here, instead of the previous biconvex section, in order to simplify the calculations by the shock-expansion method.

As indicated from the plot of lift coefficient and angle of attack, the three theories give approximately the same lift-curve slope, at least at small angles. A curve through the experimental points, taken again from the results of Ferri (reference 16), would have a slope about 10 percent less than the common theoretical value. This reduction is due to the shock-wave, boundary-layer interaction previously discussed. With regard to the angle of zero lift, the linear theory shows a value of exactly zero. The higher-order theories show a small positive value in agreement with experiment. (This experimental result, incidentally, is in direct contrast with the result in subsonic flow, where positive camber leads to a negative angle for zero lift.) In general, it may be said that the check between theory and experiment with regard to lift is within acceptable practical limits.

The agreement with regard to pitching moment is generally less satisfactory. In figure 6 the moment coefficient of the double-wedge airfoil - for moments taken about the midchord point - is plotted as a function of the lift coefficient. The inclination of the moment curves toward the right may be taken as an approximate measure of the displacement of the aerodynamic center forward of the midchord. The experimental moment coefficients are seen to be more positive than the theoretical at all lift coefficients. A straight line through the experimental data would indicate a position of the aerodynamic center forward of the midchord by about 9 percent of the airfoil chord. This displacement is significantly greater than the theoretical displacement of zero according to the linear theory or of 4 percent according to the second-order and shock-expansion theories. Both the general positive shift in the experimental moment coefficients and the relatively forward displacement of the aerodynamic center are attributable to shock-wave, boundary-layer interaction on the upper surface near the trailing edge.

Drag results for the double-wedge airfoil are shown in figure 7 as a function of the lift coefficient. Theory indicates that the variation of pressure drag with lift is essentially parabolic - exactly so in the case of the linear and second-order theories, nearly so in the case of the shock-expansion method. The second-order and shock-expansion theories give virtually coincident curves. It is seen that the experimental data agree fairly closely with these latter results. The exact agreement in the magnitude of the minimum drag is at first surprising. The effect of skin friction, which is completely neglected in the theory, would be expected to raise the measured minimum drag relative to the theoretical value. This tendency is opposed, however, by the unexpectedly high pressures in the vicinity of the trailing edge as the result of shock-wave, boundary-layer interaction. These two effects are probably compensating in the present case. Such compensation is not to be expected, however, on all airfoils or at all Mach numbers and Reynolds numbers.

The results of the foregoing figures are all for a single Mach number. Figure 8 illustrates the typical effect of variation in Mach number upon a given section characteristic, in this case the drag coefficient at zero angle of attack. The theoretical curves show an increase in the pressure drag coefficient as the Mach number decreases toward unity. (The linear and second-order theories give identical results in the present case, though this fact is not always true.) The two available experimental points confirm the theoretical tendency. The theoretical results are, as previously implied, valid down to the Mach number at which the flow behind the leading-edge shock wave becomes subsonic. Below this point, the problem is one of mixed subsonic and supersonic flow; the theoretical solutions to this problem are only now being developed.

CONCLUDING REMARKS

Only a brief outline of existing knowledge regarding the basic two-dimensional wing problem at supersonic speeds has been presented. Many subsidiary problems have been studied on the basis of the available theories, including the effects of systematic variations in airfoil shape (reference 17), the properties of flaps (reference 18), the influence of sweepback for cases in which two-dimensional theory is applicable (reference 19), and the characteristics of two-dimensional biplanes (references 20 and 21). For many such problems, valuable results have been obtained with one or another of the inviscid theories, depending upon the degree of accuracy required. In other cases, however, such as those concerning the determination of the optimum airfoil shape for a given operating condition, consideration of the effects of viscosity and the boundary layer is essential (reference 22). In the study of the effects of viscosity and the boundary layer, in particular, there is an opportunity for much valuable research.

APPENDIX

SYMBOLS

C_1, C_2	coefficients in series expansion for P
c_l	section lift coefficient
$c_{m_{c/2}}$	section pitching-moment coefficient for moments about the midchord point
c_d	section drag coefficient
$c_{d_{\alpha=0}}$	section drag coefficient at zero angle of attack
M_o	free-stream Mach number
p	local static pressure at point on airfoil
P	local pressure coefficient $\left(\frac{p - p_o}{q_o}\right)$
p_o	free-stream static pressure
q_o	free-stream dynamic pressure
α	angle of attack
γ	ratio of specific heats of gas $\left(c_p/c_v\right)$
c_p	specific heat at constant pressure
c_v	specific heat at constant volume
η	local inclination of surface of airfoil measured relative to free-stream direction

REFERENCES

1. Liepmann, Hans Wolfgang, and Puckett, Allen E.: Introduction to Aerodynamics of a Compressible Fluid. John Wiley & Sons, Inc., 1947.

2. Taylor, G. I., and Maccoll, J. W.: The Mechanics of Compressible Fluids. Vol. III of Aerodynamic Theory, div. H, W. F. Durand, ed., Julius Springer (Berlin), 1935, pp. 209-250.

3. Sauer, Robert: Theoretical Gas Dynamics. Edwards Brothers, Inc. (Ann Arbor, Mich.), 1947.

4. Von Kármán, Theodore: Supersonic Aerodynamics - Principles and Applications. Jour. Aero. Sci., vol. 14, no. 7, July 1947, pp. 373-409.

5. Busemann, A.: Aerodynamischer Auftrieb bei Uberschallgeschwindigkeit. Luftfahrtforschung, Bd. 12, Nr. 6, Oct. 3, 1935, pp. 210-220. (Available as British A.R.C. 2844, Ae. Techl. 1201, Feb. 3, 1937.)

6. Laitone, Edmund V.: Exact and Approximate Solutions of Two-Dimensional Oblique Shock Flow. Jour. Aero. Sci., vol. 14, no. 1, Jan. 1947, pp. 25-41.

7. Lighthill, M. J.: Two-Dimensional Supersonic Airfoil Theory. R. & M. No. 1929, British A.R.C., 1944.

8. The Staff of the Ames 1- by 3-Foot Supersonic Wind-Tunnel Section: Notes and Tables for Use in the Analysis of Supersonic Flow. NACA TN No. 1428, 1947.

9. Moeckel, W. E., and Connors, J. F.: Charts for the Determination of Supersonic Air Flow against Inclined Planes and Axially Symmetric Cones. NACA TN No. 1373, 1947.

10. Ivey, H. Reese, Stickle, George W., and Schuettler, Alberta: Charts for Determining the Characteristics of Sharp-Nose Airfoils in Two-Dimensional Flow at Supersonic Speeds. NACA TN No. 1143, 1947.

11. Edmonson, N., Murnaghan, F. D., and Snow, R. M.: The Theory and Practice of Two-Dimensional Supersonic Pressure Calculations. Bumblebee Rep. No. 26, The Johns Hopkins Univ., Appl. Phys. Lab., Dec. 1945.

12. Ackeret, J.: Air Forces on Airfoils Moving Faster Than Sound. NACA TM No. 317, 1925.

13. Taylor, G. I.: Applications to Aeronautics of Ackeret's Theory of Aerofoils Moving at Speeds Greater Than That of Sound. R. & M. No. 1467, British A.R.C., 1932.

14. Busemann, A., and Walchner, O.: Airfoil Characteristics at Supersonic Speeds. R.T.P. Translation No. 1786, British Ministry of Aircraft Production. (From Forschung auf dem Gebiete des Ingenieurwesens, March-April, 1933, vol. 4, pp. 87-92.)

15. Lock, C. N. H.: Examples of the Application of Busemann's Formula to Evaluate the Aerodynamic Force Coefficients on Supersonic Aerofoils. R. & M. No. 2101, British A.R.C., 1944.

16. Ferri, Antonio: Experimental Results with Airfoils Tested in the High-Speed Tunnel at Guidonia. NACA TM No. 946, 1940.

17. Ivey, H. Reese: Notes on the Theoretical Characteristics of Two-Dimensional Supersonic Airfoils. NACA TN No. 1179, 1947.

18. Collar, A. R.: Theoretical Forces and Moments on a Thin Aerofoil with Hinged Flap at Supersonic Speeds. R. & M. No. 2004, British A.R.C., 1943.

19. Ivey, H. Reese, and Bowen, Edward N., Jr.: Theoretical Supersonic Lift and Drag Characteristics of Symmetrical Wedge-Shape-Airfoil Sections as Affected by Sweepback outside the Mach Cone. NACA TN No. 1226, 1947.

20. Lighthill, M. J.: A Note on Supersonic Biplanes. R. & M. No. 2002, British A.R.C., 1944.

21. Moeckel, W. E.: Theoretical Aerodynamic Coefficients of Two-Dimensional Supersonic Biplanes. NACA TN No. 1316, 1947.

22. Ivey, H. Reese, and Klunker, E. Bernard: Considerations of the Total Drag of Supersonic Airfoil Sections. NACA TN No. 1371, 1947.

BIBLIOGRAPHY

Ferri, A.: Experiments at Supersonic Speed on a Biplane of the Busemann Type. R.T.P. Translation No. 1407, British Ministry of Aircraft Production. (From Atti di Guidonia, No. 37-38, 1940, pp. 517-557.)

Hilton, W. F., and Pruden, F. W.: Subsonic and Supersonic High Speed Tunnel Tests of a Faired Double Wedge Aerofoil. R. & M. No. 2057, British A.R.C., 1943.

Hooker, S. G.: The Pressure Distribution and Forces on Thin Airfoil Sections Having Sharp Leading and Trailing Edges, and Moving with Speeds Greater Than That of Sound. R. & M. No. 1721, British A.R.C., 1936.

Kahane, A., and Lees, Lester: The Flow at the Rear of a Two-Dimensional Supersonic Airfoil. Jour. Aero. Sci., vol. 15, no. 3, March 1948, pp. 167-170.

Lighthill, M. J.: The Conditions behind the Trailing Edge of the Supersonic Aerofoil. R. & M. No. 1930, British A.R.C., 1944.

Stanton, T. E.: A High Speed Wind Channel for Tests on Aerofoils. R. & M. No. 1130, British A.R.C., 1928.

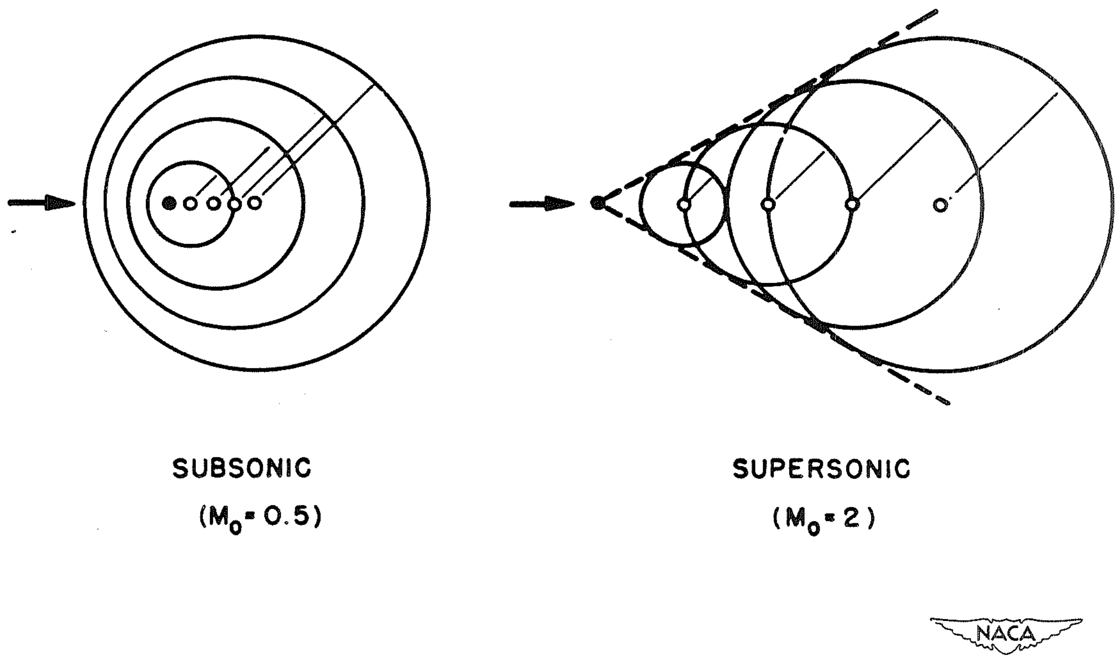

Figure 1.- Disturbance point in subsonic flow and supersonic flow.

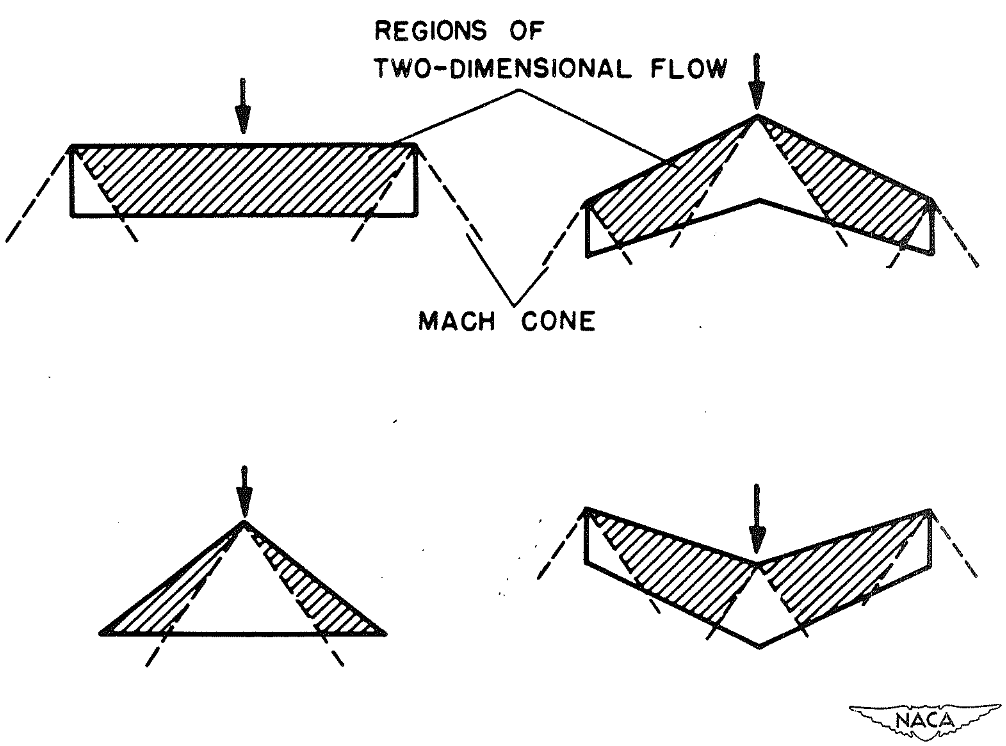

Figure 2.- Regions of two-dimensional flow.

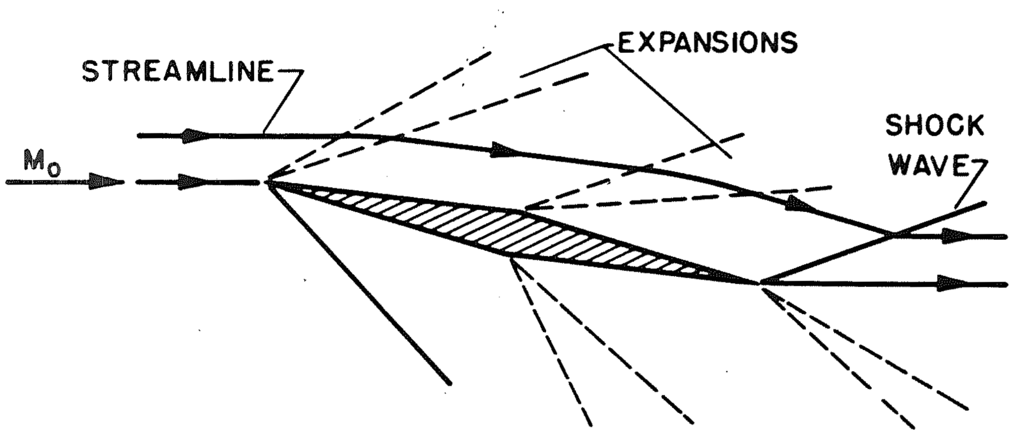

Figure 3.- Idealized flow pattern about a double-wedge section at $M_0 \approx 2$.

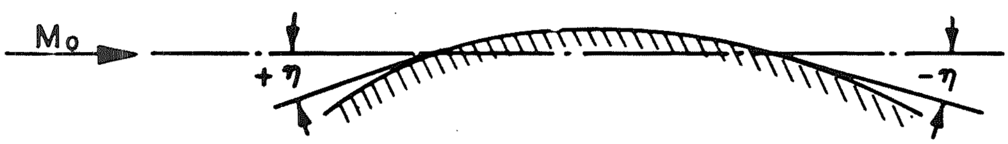

$$P = \frac{p - p_0}{q_0} = C_1 \eta + C_2 \eta^2 + \cdots \qquad (1)$$

WHERE

$$C_1 = \frac{2}{\sqrt{M_0^2 - 1}} \qquad \text{(ACKERET)} \qquad (2)$$

$$C_2 = \frac{(\gamma + 1) M_0^4 - 4 (M_0^2 - 1)}{2 (M_0^2 - 1)^2} \qquad \text{(BUSEMANN)} \qquad (3)$$

Figure 4.- Basic equations for linear and second-order theories.

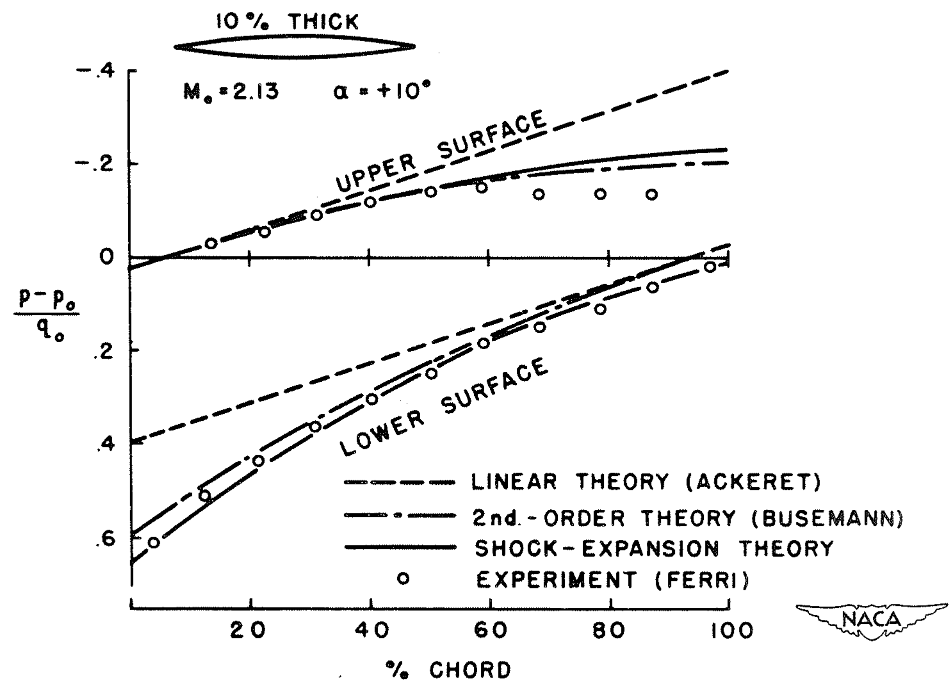

Figure 5.- Pressure distribution for symmetrical biconvex section.

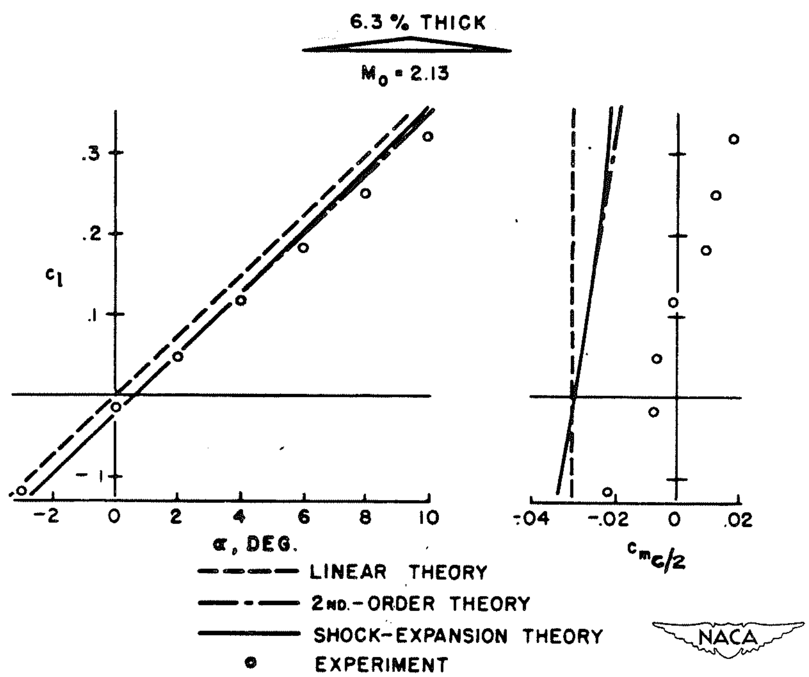

Figure 6.- Lift and pitching moment for cambered double-wedge section.

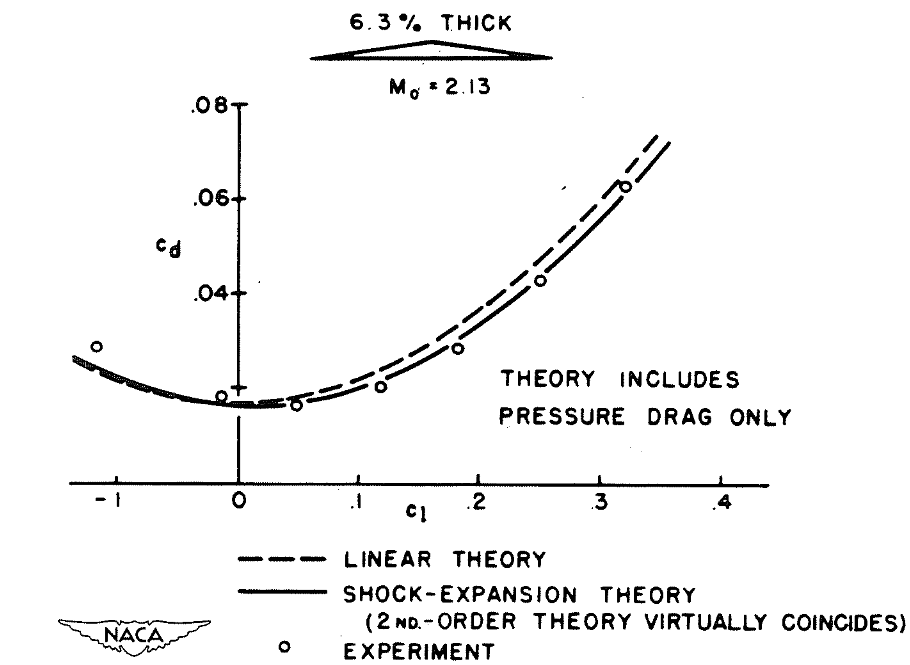

Figure 7.- Drag for cambered double-wedge section.

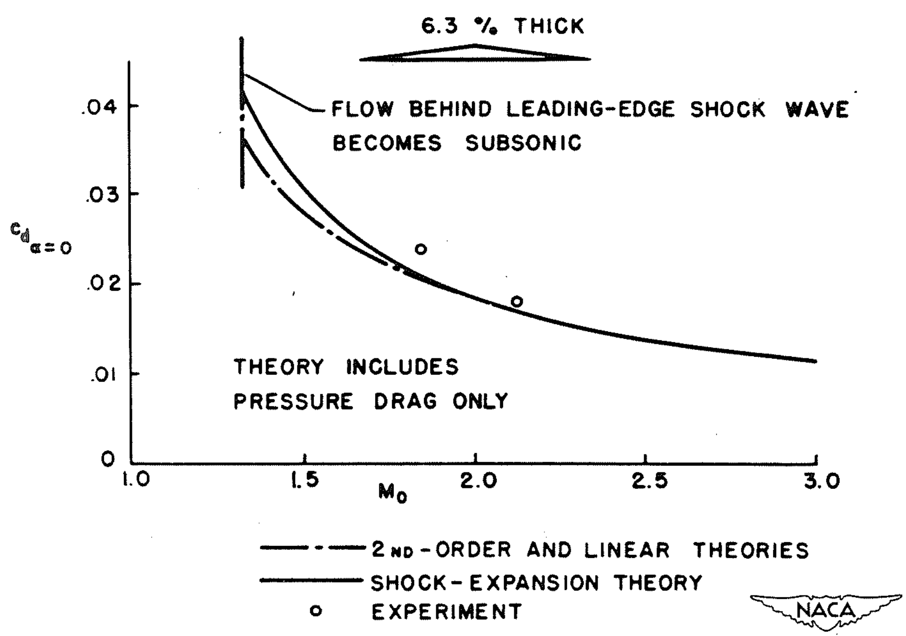

Figure 8.- Variation with Mach number of drag at zero angle of attack.